ON THE HEATING EFFICIENCY DERIVED FROM OBSERVATIONS OF YOUNG SUPER STAR CLUSTERS IN M82

Sergiy Silich[1], Guillermo Tenorio-Tagle[1], Ana Torres-Campos[1], Casiana Muñoz-Tuñón[2], Ana Monreal-Ibero[2,3], and Veronica Melo[2]

[1] Instituto Nacional de Astrofísica Optica y Electrónica, AP 51, 72000 Puebla, Mexico; silich@inaoep.mx
[2] Instituto de Astrofísica de Canarias, E 38200 La Laguna, Tenerife, Spain; cmt@ll.iac.es
[3] European Organisation for Astronomical Research in the Southern Hemisphere, Karl-Schwarzschild-Strasse 2, D-85748 Garching bei München, Germany

ABSTRACT

Here, we discuss the mechanical feedback that massive stellar clusters provide to the interstellar medium of their host galaxy. We apply an analytic theory developed in a previous study for M82-A1 to a sample of 10 clusters located in the central zone of the starburst galaxy M82, all surrounded by compact and dense H II regions. We claim that the only way that such H II regions can survive around the selected clusters, is if they are embedded into a high-pressure ISM and if the majority of their mechanical energy is lost within the star cluster volume via strong radiative cooling. The latter implies that these clusters have a low heating efficiency, η, and evolve in the bimodal hydrodynamic regime. In this regime, the shock-heated plasma in the central zones of a cluster becomes thermally unstable, loses its pressure and is accumulated there, whereas the matter injected by supernovae and stellar winds outside this volume forms a high-velocity outflow—the star cluster wind. We calculated the heating efficiency for each of the selected clusters and found that in all cases it does not exceed 10%. Such low heating efficiency values imply a low mechanical energy output and the impact that the selected clusters provide to the ISM of M82 is thus much smaller than what one would expect using stellar cluster synthetic models.

Key words: galaxies: individual (M82) – galaxies: star clusters – H II regions – ISM: bubbles – ISM: kinematics and dynamics

1. INTRODUCTION

It is a common belief that massive star clusters return a significant fraction of their stellar mass to the interstellar medium (ISM). This is thought to be done in a violent manner that deeply affects the structure of the interstellar gas and in the case of starburst galaxies, this may even result in the channeling of the processed material into the intergalactic space (see, for instance, Tenorio-Tagle et al. 2003; Cooper et al. 2008, and references therein). The general consensus is that within the volume occupied by superstar clusters (SSCs), the kinetic energy supplied by massive stars in the form of stellar winds and supernovae (SNe) explosions is there in situ thermalized. This results in a high-temperature ($T \sim 10^7$ K) plasma, with a large thermal pressure that highly exceeds that in the ambient ISM, and this provokes the exit of the thermalized ejecta out of the cluster as a supersonic star cluster wind (Chevalier & Clegg 1985). The cluster winds shape the ISM by generating large-scale superbubbles. These shock and displace the surrounding ISM while locking it into large expanding shells that are able to cool down by radiation in a short characteristic timescale, while the much lower density shock-heated wind gas, which fills the superbubble interior, remains hot for a considerably longer time (Weaver et al. 1977; Mac Low & McCray 1988; Tenorio-Tagle et al. 2006) and promotes the growth of the superbubble. This shocked wind plasma has been detected around OB-associations and stellar clusters as a soft X-ray emitter (see, for example, Chu et al. 1995; Stevens & Hartwell 2003; Silich et al. 2005, and references therein), whereas the outer shells have been traced in 21 cm (Puche et al. 1992; Ehlerová et al. 2004) or as photoionized engulfing filaments, if in the presence of a strong Lyman continuum radiation (Meaburn 1980; Lozinskaya 1992, and references therein). The size and interior pressure

of superbubbles in the case of a homogeneous interstellar gas distribution (see Mac Low & McCray 1988; Bisnovatyi-Kogan & Silich 1995 and references therein) are

$$R_{sb} = \left(\frac{375(\gamma - 1)}{28(9\gamma - 4)\pi} \right)^{1/5} \left(\frac{L_{\rm out}}{\rho_{\rm ISM}} \right)^{1/5} t^{3/5}, \qquad (1)$$

$$P_{sb} = 7\rho_{\rm ISM} \left[\frac{3(\gamma - 1)}{700(9\gamma - 4)\pi} \frac{L_{\rm out}}{\rho_{\rm ISM}} \right]^{2/5} t^{-4/5}, \qquad (2)$$

where $\gamma = 5/3$ is the ratio of specific heats, R_{sb} is the outer shell radius, P_{sb} is the pressure in the shock-heated wind region, $L_{\rm out}$ is the star cluster mechanical energy output, $\rho_{\rm ISM}$ is the interstellar gas density, and t is the evolutionary time. The superbubbles are supposed to expand until they acquire pressure equilibrium with the surrounding medium ($P_{sb} = P_{\rm ISM}$), when

$$R_{sb} = (7\gamma)^{3/4} \left[\frac{3(\gamma - 1)}{28(9\gamma - 4)\pi} \frac{L_{\rm out}}{\rho_{\rm ISM} a_{\rm ISM}^3} \right]^{1/2}$$

$$= 637 \left(\frac{L_{38}}{n_{\rm ISM} a_{10}^3} \right)^{1/2} \text{ pc}, \qquad (3)$$

where $n_{\rm ISM}$ is the interstellar gas number density, L_{38} is the mechanical energy output in units of 10^{38} erg s^{-1}, and a_{10} is the sound speed in the ISM in units of 10 km s^{-1}.

However, as noted by Silich et al. (2007), this cannot be the whole story. The observed properties of the H II region associated with the massive (1.3×10^6 $M_{\odot}$), young (age $\sim$ 6 Myr) and thus powerful (with a mechanical luminosity, $L_{\rm mech} \approx 2.5 \times 10^{40}$ erg s^{-1}) SSC M82-A1 (Smith et al. 2006) are

not consistent with the interstellar bubble model (Equations (1)–(3)). The associated minute, low-mass ($M_{\mathrm{H\,II}} \approx 5 \times 10^3 \ M_\odot$), although dense ($n_{\mathrm{H\,II}} \approx 1800 \ \mathrm{cm}^{-3}$), H II region presents a radius ($R_{\mathrm{H\,II}} \approx 4.5$ pc) much smaller than that predicted by Equations (1) and (3). It seems surprising that M82-A1 and other young and massive clusters in M82 (Melo et al. 2005), NGC 3351 (Hägele et al. 2007), and in other galaxies are surrounded by compact, low-mass (see Table 2 below) H II regions despite the powerful mechanical energy output predicted for the clusters by stellar evolution synthesis models.

Silich et al. (2007) suggested that in this case clearly only a fraction of the star cluster mechanical luminosity is converted into the energy of the outflowing plasma whereas the rest ought to be lost due to strong radiative cooling. They also developed an analytic and semianalytic model, which led to obtain the value of the heating efficiency η, the parameter which links the star cluster mechanical luminosity with the actual thermal energy that is deposited into the star cluster volume. The models reveal the value of the heating efficiency by fitting the ionized gas number density and radius of the compact H II region detected around a massive star cluster. The results led to a low heating efficiency ($\eta < 10\%$) in the case of M82-A1.

Here, we extend the analysis of Silich et al. (2007) to a sample of 10 SSCs selected from the list of Melo et al. (2005), in order to reveal their heating efficiency, and thus the energy that these clusters return to the ISM of M82.

Sections 2 and 3 discuss the hydrodynamics of SSCs, the model assumptions, and present the equations used in order to obtain the heating efficiency. The sample of the selected clusters is presented in Section 4. We apply our model to each of the selected clusters and discuss our results in Section 5.

2. THE HEATING EFFICIENCY IN SSCs

The hydrodynamics of the matter returned by stellar winds and SN explosions within the cluster volume has been approximated assuming first that the sources are equally spaced within a spherical volume of radius R_{SC}. In the pioneer adiabatic approach of Chevalier & Clegg (1985), the kinetic energy supplied by the evolving massive stars, L_{mech}, has been assumed to be completely converted into thermal energy of the hot plasma. The strong pressure gradient generated by the deposited matter, forces then the gas velocity to increase almost linearly from 0 km s^{-1} at the star cluster center to its sound speed at the cluster edge. Once the gas streams out of the cluster, it rapidly acquires its terminal speed ($v_{A\infty} \sim 2c_{\mathrm{SC}}$), while its density and temperature drop as r^{-2} and $r^{-4/3}$, respectively.

More recently, Silich et al. (2004), Tenorio-Tagle et al. (2005, 2007), and Wünsch et al. (2008) recognized that the adiabatic assumption is not valid in the case of massive and compact star clusters and developed a radiative star cluster wind model, which takes into consideration the energy losses that occur in the hot thermalized plasma. They found a threshold line, $L_{\mathrm{crit}}(R_{\mathrm{SC}})$ in the L_{mech}–R_{SC} parameter space. The radiative solution is in excellent agreement with Chevalier & Clegg's (1985) results in the case of low-mass clusters, when $L_{\mathrm{mech}} \ll L_{\mathrm{crit}}$. However, strong radiative cooling modifies essentially the temperature distribution outside the cluster when the star cluster mechanical luminosity approaches the threshold value, $L_{\mathrm{mech}} \lesssim L_{\mathrm{crit}}$. When the mechanical luminosity of the considered clusters exceeds the threshold value, L_{crit}, catastrophic cooling sets in within the central zones of the cluster, which results into a bimodal flow regime. In this case, the stagnation radius, R_{st}, moves out of the cluster center and splits the cluster volume into two distinct zones. In the inner zone, $r < R_{\mathrm{st}}$, strong radiative cooling promotes frequent thermal instabilities in the injected gas, reducing significantly the pressure gradient and thus the outward acceleration. Strong radiative cooling thus leads to the accumulation of the matter injected within the volume defined by the stagnation surface. In the outer zone, $R_{\mathrm{st}} < r < R_{\mathrm{SC}}$, despite radiative cooling, the pressure gradient remains sufficient to drive the injected matter away from the cluster, as a strongly radiative stationary wind.

The detail physics during the thermalization process are however not well understood. In the original paper of Chevalier & Clegg (1985), it was assumed that the amount of the deposited thermal energy per unit volume, q_e, is identical to the rate of mechanical energy released by massive stars: $q_e = q_{\mathrm{mech}}$. However, Stevens & Hartwell (2003) found that this assumption is not in good agreement with the spectra of the diffuse X-ray emission detected in a number of nearby massive clusters. Bradamante et al. (1998) and Recchi et al. (2001), who studied the chemical and dynamical evolution of blue compact galaxies, also claimed that only a few percent of the energy deposited by SNe type II provides the energetics of the host galaxy ISM, while the rest is radiated away. It is therefore highly desirable to link the value of the heating efficiency with stellar clusters observable quantities.

A firm evidence for an incomplete transformation of the star cluster mechanical luminosity into the energy of the star cluster wind was obtained by Smith et al. (2006), who provided detailed photometric and spectral analysis of the massive, young SSC M82-A1 and its associated H II region. This led them, as well as to Silich et al. (2007), to claim that the energy q_e represents only a small fraction of the mechanical energy provided by massive stars: $q_e = \eta q_{\mathrm{mech}}$, with $\eta \ll 1$. The physical justification for this parameter comes from the fact that strong radiative cooling may take place during the process of thermalization either because of an enhanced gas metallicity, resultant from SN explosions, or because of the large densities within the shock-heated zones between neighboring massive stars, before the newly injected matter joins the flow (Wünsch et al. 2007; Silich et al. 2007). In this case, only a fraction of the mechanical energy supplied by the collection of massive stars is shared by the matter within the cluster volume and thus the actual thermal energy given to the injected gas is smaller than that provided by the collection of massive stars. This is particularly important in the case of massive ($M_{\mathrm{SC}} \geqslant 10^5 \ M_\odot$) and compact ($R_{\mathrm{SC}} \sim$ a few parsecs) clusters which present a large massive star number density, $N_\star$, and a small mean separation between them $\Delta R = N_\star^{-3} \ll 1$ pc.

Indeed, the multiple interactions expected between supersonic stellar winds and the SNe ejecta in such compact and massive clusters are similar to those occurring in colliding wind binaries that lead to a shock-heated plasma that effectively radiates in the soft X-ray regime. Luo et al. (1990) and Stevens et al. (1992) found that in the case of colliding wind binaries the amount of energy radiated away from the shock-heated zone, L_{lost}, depends on the binary separation. It scales as $L_{\mathrm{lost}} \sim \Delta R^{-1}$ in the quasi-adiabatic regime and increases when radiative cooling in the shock-heated zone is taken into consideration. In the case of a dense stellar cluster the kinetic energy placed by massive stars interacts with that deposited by multiple nearby neighbors. This suggests that the energy, which actually drives the star cluster outflow, is smaller than the total provided by the massive

stars within the cluster volume, particularly if one accounts for the large metallicities expected from SNe.

In the semianalytic models, all uncertainties dealing with the distribution of massive stars and the collisions between nearby supersonic flows and thus the sudden loss of energy, are accounted for by the parameter η, known as the heating efficiency. The fraction of energy that a star cluster returns to the ambient interstellar gas strongly depends on this parameter. Thus, η defines the mechanical feedback that star clusters provide to the ISM of their host galaxy.

3. THE PRESSURE-CONFINED WIND MODEL

The pressure-confined wind model (Silich et al. 2007) suggests that the combination of two factors is crucial in order to produce the compact and dense H II regions able to survive around powerful young clusters. These are a low heating efficiency and a large thermal pressure, P_{ISM}, in the surrounding ISM, which leads to a pressure-confined bubble configuration. Thus, in this model the size of the standing H II region depends critically on the balance between P_{ISM} and the wind ram pressure at the reverse shock position ($P_{ram} = P_{ISM}$). In this case, the structure of the outflow can be derived analytically from a set of equations that consider: conservation of mass, photoionization balance, pressure equilibrium, and the fast radiative cooling that occurs within the star cluster volume and on its wind. Our set of equations is such that if the parameters of the driving stellar cluster: its mass (M_{SC}), radius (R_{SC}), the number of ionizing photons (N^{SC}) are known, one can match the model predicted radius ($R_{H II}$) and gas number density ($n_{H II}$) of the associated H II region with the observed values. In this approach, one can find the value of the heating efficiency from a nonlinear algebraic equation which relates η with the host cluster and the associated H II region parameters (see Silich et al. 2007):

$$1 - \frac{\left(4\pi P_{ISM} V_{A\infty}^2 R_{H II}^2\right)^{1/2}}{\left(4 L_{crit} L_{SC} V_\infty^2\right)^{1/4}} \left[\left(1 - \frac{3 f_t N^{SC}}{4\pi \beta n_{H II}^2 R_{H II}^3}\right)^{1/3} \right.$$
$$\left. - \frac{9}{512} \frac{f_\lambda \mu_i^2 V_\infty^5}{P_{ISM} R_{H II} \Lambda_s} \right] = 0, \quad (4)$$

where $V_{A\infty} = (2 L_{SC}/\dot{M}_{SC})^{1/2}$ is the adiabatic wind terminal speed, L_{SC} and $\dot{M}_{SC}$ are the star cluster mechanical luminosity and the mass input rate, respectively, Λ_s is the value of the cooling function at the reverse shock radius, β is the recombination coefficient to all but the ground level, $f_\lambda = 0.3$ is a fiducial coefficient, and f_t is the fraction of ionizing photons, which reaches the outer standing gaseous shell. Note that Equation (4) is only valid in the bimodal parameter space, i.e., it can only be applied to clusters with a mechanical power that exceeds the threshold value L_{crit}, and carries a strong implicit dependence on η via the threshold mechanical luminosity, L_{crit} and the star cluster wind terminal speed, V_∞ (see Wünsch et al. 2007; Silich et al. 2007):

$$L_{crit} = \frac{3\pi \eta \alpha^2 \mu_i^2 R_{SC} V_{A\infty}^4}{2\Lambda_{st}} \left(\frac{\eta V_{A\infty}^2}{2} - \frac{c_{st}^2}{\gamma - 1} \right), \quad (5)$$

$$V_\infty = [2/(\gamma - 1)]^{1/2} c_{st}, \quad (6)$$

where $\alpha = 0.28$ and $\mu_i = 14 m_H/11$ is the mean mass per ion. Λ_{st} and c_{st} are the values of the cooling function and the

speed of sound at the stagnation point, both are functions of temperature at the stagnation radius, T_{st}, which strongly depends also on η. We obtain the value of T_{st} from the condition that the stagnation pressure reaches the maximum possible value and thus $dP_{st}/dT_{st} = 0$ (Tenorio-Tagle et al. 2007):

$$\left(\frac{\eta V_{A\infty}^2}{2} - \frac{c_{st}^2}{\gamma - 1} \right) \left(1 - \frac{T_{st}}{2\Lambda} \frac{d\Lambda}{dT_{st}} \right) - \frac{1}{2} \frac{c_{st}^2}{\gamma - 1} = 0. \quad (7)$$

Note that the calculated heating efficiency does not depend significantly on the parameter f_t. Hereafter we shall assume that $f_t = 0.5$ and $V_{A\infty} = 1000$ km s^{-1}.

In order to relate the star cluster mass with the star cluster mechanical luminosity we use a relation, which approximates the results of the Starburst 99 synthesis model for coeval clusters with a Salpeter initial mass function with sources between 1 $M_\odot$ and 100 $M_\odot$ and ages in the range $\sim$ 4–12 Myr (Leitherer et al. 1999):

$$L_{SC} = 3 \times 10^{40} \left(\frac{M_{SC}}{10^6 \, M_\odot} \right) \text{ erg s}^{-1}. \quad (8)$$

Equation (4) presents only a weak dependence on L_{SC} and thus deviations of the star cluster mechanical luminosity from the assumed constant value do not affect the final results significantly.

Thus, in this approach one can obtain the heating efficiency η directly from the observed parameters of the stellar cluster and its associated H II region: M_{SC}, R_{SC}, N^{SC}, $R_{H II}$, and $n_{H II}$ by solving Equation (4).

4. A SAMPLE OF CLUSTERS IN M82

In order to learn how efficient the conversion of the star cluster mechanical luminosity into the wind driving energy is, one needs a sample of clusters whose masses, sizes, and Lyman continuum radiation are known together with the radius and density of their adjacent H II regions. Most of these parameters can be obtained from the photometric sample of Melo et al. (2005) who cataloged 197 young superstellar clusters in the central zone of the galaxy M82. The only parameter, which is required by Equation (4) and which Melo et al. (2005) did not obtain, is the density of the ionized gas in the H II regions. We obtain this quantity from *Potsdam Multi Aperture Spectrophotometer* (PMAS; Roth et al. 2005) observations at the 3.5 m telescope in Calar Alto. PMAS is a very versatile instrument, with several working modes. Here, we used its lens array (LARR) which is made out of 16 × 16 square elements. We observed the nuclear region of M82 using two continuous fields with the spatial sampling of 0''5 × 0''5 and thus, covering a field of view of 8''0 × 8''0 per pointing. Two different sets of observations were provided. A set of data with low spectral resolution, covering the whole optical spectral range was obtained in the service mode on the 3rd and 4th of 2005 June while that with a high spectral resolution on the 2nd of 2005 February. Both sets of data were taken under nonphotometric conditions. Seeing ranged typically between 1''3 and 1''6. Line profiles were fitted using Gaussian functions. This procedure was done in an automatic way using the IDL-based routine MPFITEXPR implemented by Markwardt (2009)[4] checking each fit, afterward. A single Gaussian fit was enough in order to reproduce the observed profiles. For each set of lines, wavelength differences between

---

[4] See http://purl.com/net/mpfit
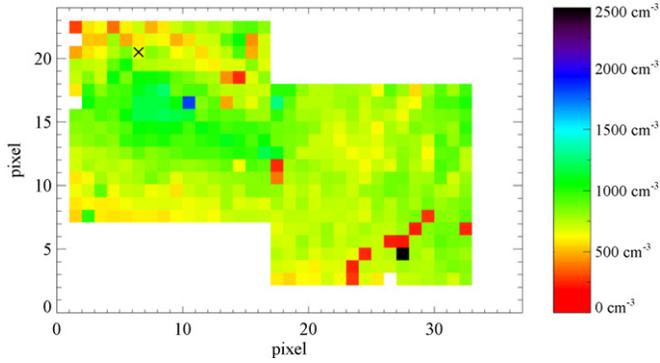
Figure 1. Ionized gas density distribution derived from the PMAS observations. The range of densities is coded by color scale on the right of the panel. Positions of different points in the field of view of PMAS are given in pixels. The position of the M82-A1 cluster is marked with a cross symbol.

Figure 2. *HST* WFPC2 image of the central zone of M82 taken in the F656N filter. The selected clusters are shown as green dots. The position of the M82-A1 cluster is used as a reference point and is marked with a red plus. The dashed lines outline the field of view of PMAS.

Table 1
Selected Clusters

Cluster	ID Melo et al. (2005)	Zone	ID Mayya et al. (2008)
(1)	(2)	(3)	(4)
1	20	SW	178N
2	52	SE	47N
3	12	SE	13N
4	58	SE	34N
5	14	SE	20N
6	59	SE	45N
7	3	NE	71N
8	72	SE	200N
9	81	SE	32N
10	75	SE	28N

them were fixed and the same line width was assumed. Then the intensity maps of Hα and S II lines were produced.

Our field of view includes region A (O'Connell & Mangano 1978) of the central zone as well as a highly extincted heart-shaped region toward the west. In order to localize the selected clusters in the PMAS map, the resolution of the *Hubble Space Telescope* (*HST*) image was degraded to 0″.506 pixel^{-1}, which is almost identical to that of PMAS (0″.5 pixel^{-1}) and a new, low-resolution *HST* Hα map of M82 nuclear region was generated. As we did not have absolute astrometry and in order to use the two observing data sets, the low-resolution *HST* and the PMAS Hα maps were compared and displaced until reaching the highest cross correlation coefficient (Russ 2002, p. 527). Then the electron density, $n_{\rm H\,II}$, was derived (see Table 2) from a map of the [S II] λ6717/[S II] λ6731 line ratio using the task `temden`, based on the `fivel` program (Shaw & Dufour 1995), included in the IRAF package `nebular` and assuming an electronic temperature of 10,000 K (see Figure 1).

We use the electron density values and the photoionization balance equation in order to estimate the masses of the associated H II regions:

$$M_{\rm H\,II} = \frac{\mu_i N^{\rm SC}}{\beta n_{\rm H\,II}}, \qquad (9)$$

where μ_i is the mean mass per ion and $\beta = 2.59 \times 10^{-13}$ cm^{-3} s^{-1} is the recombination coefficient to all but the ground level.

Eighty four out of the 197 clusters found by Melo et al. (2005) are located in the area observed with PMAS. From the large sample of young SSCs cataloged by Melo et al. (2005) we have selected a subsample which follows the criteria that the radius of the H II region (the one defined in the Hα *HST* images) lies clearly outside the volume occupied by the SSCs themselves (radius taken from the continuum *HST* images). In this way we selected a total of 21 objects. We then compared our list of cluster candidates with that of Mayya et al. (2008), who used the *HST* Advanced Camera for Surveys (ACS) and selected only those sources, which were simultaneously detected in three different (*B*, *V*, and *I*) filters. Only 10 counterparts for our 21 candidate clusters were found in the list of Mayya et al. (2008). We have selected these as genuine clusters for our further discussion. Figure 2 presents the location of the selected clusters within the galaxy and also outlines the area in the central zone of M82, which was observed with PMAS.

Table 1 presents the identification of the selected clusters. Here, the first column marks the clusters in our list, Columns 2 and 3 provide the star cluster and the M82 zone identification

in the sample of Melo et al. (2005), and Column 4 lists the identification number in the sample of Mayya et al. (2008).

Table 2 presents the star cluster masses and radii (Columns 2 and 3, respectively) and the number of Lyman continuum photons (Column 4) taken from Melo et al. (2005). The number densities, radii, and masses of the associated H II regions are given in Columns 5, 6, and 7, respectively. Column 8 presents the calculated values of the heating efficiency and Column 9—the output mechanical luminosity normalized to the star cluster mechanical luminosity, $L_{\rm SC}$, predicted by the Starburst 99 synthetic model.

Note that the cluster radii fall into a narrow size interval, $2 < R_{\rm SC} < 6$ pc whereas their masses vary from 2×10^4 $M_\odot$ to 8×10^5 $M_\odot$. In all selected cases the resulting masses of the associated H II regions do not exceed a few thousand solar masses, just as in the case of M82-A1 whose stellar mass is $\sim 10^6$ $M_\odot$ and its associated H II region has only ~ 5000 $M_\odot$ (Smith et al. 2006).
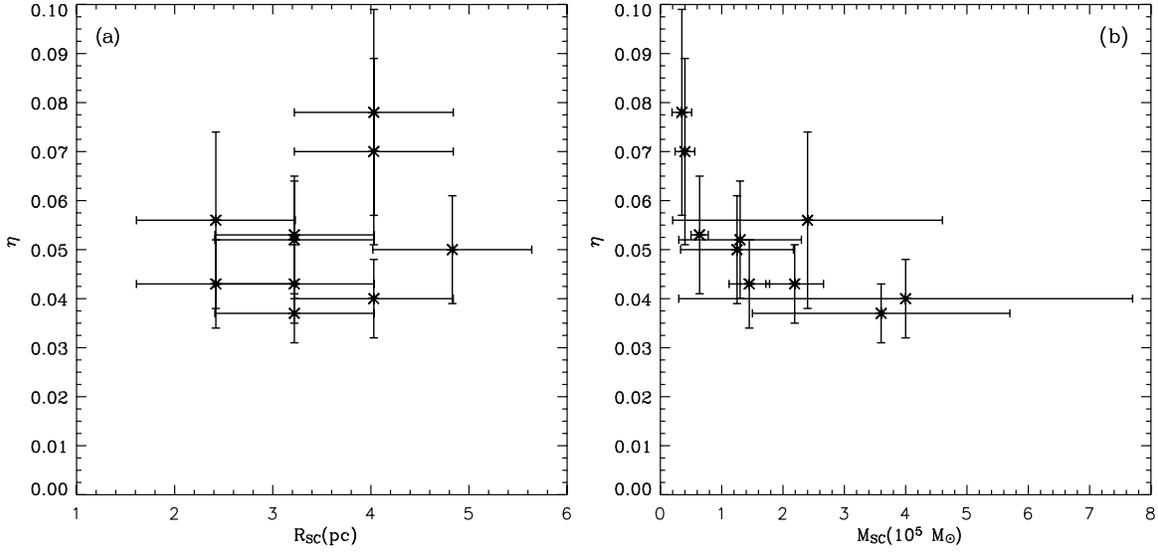
Figure 3. Calculated heating efficiency. Panels (a) and (b) present the star clusters heating efficiency as a function of star cluster radius and mass, respectively.

Table 2
Parameters of the Selected Clusters and Their H II Regions

Cluster	M_{SC} ($10^5\ M_\odot$)	R_{SC} (pc)	N^{SC} (10^{49} s^{-1})	$n_{H\,II}$ (cm^{-3})	$R_{H\,II}$ (pc)	$M_{H\,II}$ ($M_\odot$)	η (%)	L_{out}/L_{SC} (%)
(1)	(2)	(3)	(4)	(5)	(6)	(7)	(8)	(9)
1	$0.35^{\pm0.16}$	4.03	$7.1^{\pm3.7}$	$769^{\pm76}$	5.64	381.6	$7.8^{\pm2.1}$	$3.17^{\pm1.06}$
2	$0.40^{\pm0.16}$	4.03	$34.0^{\pm21.0}$	$950^{\pm51}$	4.83	1479.3	$7.0^{\pm1.9}$	$2.46^{\pm0.93}$
3	$1.25^{\pm0.92}$	4.83	$17.7^{\pm9.4}$	$706^{\pm71}$	5.64	1036.2	$5.0^{\pm1.1}$	$0.83^{\pm0.34}$
4	$0.64^{\pm0.14}$	3.22	$19.0^{\pm7.9}$	$953^{\pm81}$	4.03	824.1	$5.3^{\pm1.2}$	$1.04^{\pm0.44}$
5	$1.30^{\pm1.0}$	3.22	$15.2^{\pm8.4}$	$665^{\pm60}$	5.64	944.8	$5.2^{\pm1.2}$	$0.71^{\pm0.31}$
6	$4.00^{\pm3.7}$	4.03	$24.0^{\pm12.0}$	$886^{\pm115}$	4.83	1119.6	$4.0^{\pm0.8}$	$0.23^{\pm0.12}$
7	$2.19^{\pm0.47}$	3.22	$58.0^{\pm22.0}$	$771^{\pm170}$	4.83	3109.4	$4.3^{\pm0.8}$	$0.33^{\pm0.15}$
8	$1.45^{\pm0.33}$	2.42	$16.6^{\pm5.1}$	$1146^{\pm76}$	3.22	598.7	$4.3^{\pm0.9}$	$0.34^{\pm0.18}$
9	$3.60^{\pm2.1}$	3.22	$18.0^{\pm8.2}$	$850^{\pm145}$	4.03	875.3	$3.7^{\pm0.6}$	$0.17^{\pm0.08}$
10	$2.40^{\pm2.2}$	2.42	$24.0^{\pm15.0}$	$1163^{\pm82}$	4.83	853.0	$5.6^{\pm1.7}$	$0.53^{\pm0.28}$

Notes. Parameters of the clusters (Columns 2, 3, and 4), radii of the associated H II regions (Column 6) and uncertainties in their determination are taken from Melo et al. (2005). Ionized gas density (Column 5) was derived from PMAS observations. 1 pixel uncertainty (±0.81 pc) was adopted in the determination of all radii.

5. RESULTS AND DISCUSSION

Each of the selected clusters (see Table 2) is surrounded by a compact H II region and has all attributes required by our model. We solve Equation (4) by iteration with the relative accuracy $\Delta\eta/\eta \leqslant 10^{-5}$. Equations (5)–(7) were used every time when the iteration procedure requires new values for the threshold luminosity, L_{crit}, cooling function, Λ_{st}, and the star cluster wind terminal speed, V_∞. Our results for each of the considered clusters are shown in Table 2 (Column 8). We use the error propagation equation (Bevington & Robinson 2003, p. 41) in order to calculate the errors provided by the uncertainties in the determination of the input parameters of the model: M_{SC}, R_{SC}, N^{SC}, $R_{H\,II}$, and $n_{H\,II}$. Unfortunately, the uncertainties in the determination of the star cluster radii and sizes of the H II regions are not presented in the original paper of Melo et al. (2005). We take a 1 pixel (±0.81 pc) as a conservative estimate for the uncertainties in the measured radii.

The results of the calculations are presented in Figure 3, where the heating efficiency is presented as a function of star cluster radii and masses. It seems that there is a trend on panel (b) for the heating efficiency to be larger for less massive clusters.

However, this must be confirmed with better sets of input data. We also suggest for a future analysis that the star cluster stellar density may be a better input parameter, which combines the two major observables, the star cluster mass and radius, into a single parameter.

Figure 3 shows that the heating efficiency does not exceed 10% for all clusters in our sample. This implies that our massive and compact stellar clusters have a much reduced outflow velocity and negative feedback into the ambient ISM than what one would expect using synthetic models. Indeed, the mechanical energy output rate is

$$L_{out} = \tfrac{1}{2}\dot{M}_{out}V_\infty^2, \qquad (10)$$

where the star cluster wind terminal speed, V_∞, is defined by Equations (7) and (6) and the mass output rate, $\dot{M}_{out}$, is (Wünsch et al. 2007)

$$\dot{M}_{out} = \dot{M}_{SC}\left(\frac{L_{crit}}{L_{SC}}\right)^{1/2}. \qquad (11)$$

The critical luminosity, L_{crit}, is defined by Equation (5). The fraction of the injected mechanical energy, L_{out}/L_{SC}, that a

cluster returns to the ambient ISM thus is

$$\frac{L_{\text{out}}}{L_{\text{SC}}} = \left(\frac{L_{\text{crit}}}{L_{\text{SC}}}\right)^{1/2} \left(\frac{V_\infty}{V_{A\infty}}\right)^2 . \qquad (12)$$

The calculated mechanical energy output does not exceed a few percent of the star cluster mechanical luminosity for all selected clusters (see Table 2). Only in this way the shock-heated matter driven out as a cluster wind can cool rapidly to $T \leqslant 10^4$ K and be photoionized while a high ambient pressure prevents its expansion into the surrounding ISM.

The implication of our results, when compared with the recently inferred (Strickland & Heckman 2009) net efficiency of SN and stellar wind feedback in the nucleus of M82 ($\geqslant 30\%$), is that there is a phase, a time during which massive and compact clusters have a low heating efficiency and undergo a bimodal hydrodynamic solution returning to the ISM of their host galaxy only a small fraction of mass and mechanical energy released inside the star cluster volume. Here, we suggest that the selected young, massive clusters pass through such special phase in their hydrodynamical evolution, highlighted observationally by the presence of a compact H II region. Indeed, the relevant cluster parameters such as the energy and mass deposition rates, the mean separation between nearby energy sources, and the chemical composition of the injected matter—all change with time. This must lead to important changes in η and thus to large displacements of the threshold luminosity and noticeable changes in the rates of mass, $\dot{M}_{\text{out}}$, and energy, L_{out}, which a star cluster returns to the ISM. The time evolution of η will be the subject of a forthcoming communication.

REFERENCES

Bevington, P. R., & Robinson, D. K. 2003, Data Reduction and Error Analysis for the Physical Sciences (New York: McGraw-Hill)
Bisnovatyi-Kogan, G. S., & Silich, S. A. 1995, Rev. Mod. Phys., 67, 661
Bradamante, F., Matteucci, F., & D'Ercole, A. 1998, A&A, 337, 338
Chevalier, R. A., & Clegg, A. W. 1985, Nature, 317, 44
Chu, Y.-H., Chang, H.-W., Su, Y.-L., & Mac Low, M.-M. 1995, ApJ, 450, 157
Cooper, J. L., Bicknell, G. V., Sutherland, R. S., & Bland-Hawthorn, J. 2008, ApJ, 674, 157
Ehlerová, S., Palouš, J., & Wünsch, R. 2004, Ap&SS, 289, 279
Hägele, G. F., Díaz, A. I., Cardaci, M. V., Terlevich, E., & Terlevich, R. 2007, MNRAS, 378, 163
Leitherer, C., et al. 1999, ApJS, 123, 3
Lozinskaya, T. 1992, Supernovae and Stellar Wind in the Interstellar Medium (Melville, NY: AIP)
Luo, D., McCray, R., & Mac Low, M.-M. 1990, ApJ, 362, 267
Mac Low, M.-M., & McCray, R. 1988, ApJ, 324, 776
Markwardt, C. B. 2009, arXiv:0902.2850
Mayya, Y. D., Romano, R., Rodríguez-Merino, L. H., Luna, A., Carrasco, L., & Rosa-González, D. 2008, ApJ, 679, 404
Meaburn, J. 1980, MNRAS, 192, 365
Melo, V. P., Muñoz-Tuñón, C., Maíz-Apellániz, J., & Tenorio-Tagle, G. 2005, ApJ, 619, 270
O'Connell, R. W., & Mangano, J. J. 1978, ApJ, 221, 62
Puche, D., Westpfahl, D., Brinks, E., & Roy, J.-R. 1992, AJ, 103, 1841
Recchi, S., Matteucci, F., & D'Ercole, A. 2001, MNRAS, 322, 800
Roth, M. M., et al. 2005, PASP, 117, 620
Russ, J. C. 2002, The Image Processing Handbook (Boca Raton, FL: CRC Press)
Shaw, R. A., & Dufour, R. J. 1995, PASP, 107, 896
Silich, S., Tenorio-Tagle, G., & Añorve Zeferino, G. A. 2005, ApJ, 635, 1116
Silich, S., Tenorio-Tagle, G., & Muñoz-Tuñón, C. 2007, ApJ, 669, 952
Silich, S., Tenorio-Tagle, G., & Rodríguez González, A. 2004, ApJ, 610, 226
Smith, L. J., Westmoquette, M. S., Gallagher, J. S. III, O'Connell, R. W., Rosario, D. J., & de Grijs, R. 2006, MNRAS, 370, 513
Stevens, I. R., Blondin, J. M., & Pollock, A. M. T. 1992, ApJ, 386, 265
Stevens, I. R., & Hartwell, J. M. 2003, MNRAS, 339, 280
Strickland, D. K., & Heckman, T. M. 2009, ApJ, 697, 2030
Tenorio-Tagle, G., Muñoz-Tuñón, C., Pérez, E., Silich, S., & Telles, E. 2006, ApJ, 643, 186
Tenorio-Tagle, G., Silich, S., & Muñoz-Tuñón, C. 2003, ApJ, 597, 279
Tenorio-Tagle, G., Silich, S., Rodríguez-González, A., & Muñoz-Tuñón, C. 2005, ApJ, 628, L13
Tenorio-Tagle, G., Wünsch, R., Silich, S., & Palouš, J. 2007, ApJ, 658, 1196
Weaver, R., McCray, R., Castor, J., Shapiro, P., & Moore, R. 1977, ApJ, 218, 377
Wünsch, R., Silich, S., Palouš, J., & Tenorio-Tagle, G. 2007, A&A, 471, 579
Wünsch, R., Tenorio-Tagle, G., Palouš, J., & Silich, S. 2008, ApJ, 683, 683